Reliability-Oriented Broadcast Electrode-Addressing for Pin-Constrained Digital Microfluidic Biochips

Tsung-Wei Huang*, Tsung-Yi Ho*, and Krishnendu Chakrabarty†
*Department of Computer Science and Information Engineering, National Cheng Kung University, Tainan, Taiwan
†Department of Electrical and Computer Engineering, Duke University, Durham, NC

***Abstract*—Designs for pin-constrained digital microfluidic biochips (PDMFBs) are receiving much attention because they simplify chip fabrication and packaging, and reduce product cost. To reduce the pin count, *broadcast addressing*, by minimally grouping electrode sets with non-conflict signal merging, has emerged as a promising solution. Nevertheless, naive signal merging has the potential to cause excessive electrode actuations, which has been reported to have direct and adverse effect on chip reliability. According to recent studies, reliability is an important attribute for PDMFBs particularly developed for medical applications as it directly affects the final medical decision making. However, no research findings have been reported on the reliability problem in pin-constrained designs. To make PDMFBs more feasible for practical applications, we propose in this paper the first matching-based reliability-oriented broadcast-addressing algorithm for PDMFBs. We identify the factors that affect reliability and incorporate into the design-technique attributes that enhance reliability. Experimental results demonstrate the effectiveness of the proposed algorithm.**

I. Introduction

Recently, *droplet*-based digital microfluidic biochips (DMFBs), have emerged as a popular alternative for laboratory experiments. By controlling miniaturized and discrete liquids (i.e., droplets), DMFBs offer various advantages including high portability, high throughput, high sensitivity, less human intervention, and low sample volume consumption. Due to these advantages, practical applications such as clinical diagnostics, DNA analysis, environmental toxin monitoring, and drug discovery have been successfully realized on DMFBs [5], [12].

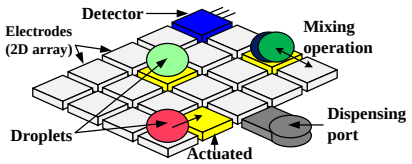

Figure 1. The schematic view of a DMFB.

Generally, a DMFB consists of a two-dimensional (2D) electrode array and peripheral devices (e.g., optical detector, dispensing port, etc.), as schematically shown in Figure 1 [12]. On a DMFB, the sample carriers, *droplets*, are controlled by underlying electrodes using electrical actuations to generate electrowetting force (i.e., a principle called electrowetting-on-dielectric or EWOD) [10]. By assigning time-varying voltage values to turn on/off electrodes, droplets can be moved around the entire 2D array to perform fundamental operations (e.g., dispensing and mixing). These operations are carried out under clock control in a *reconfigurable* manner due to their flexibility in spatial and time domain [2].

To ensure droplet control using an electrode actuation sequence corresponding to a biochemical protocol, we need to apply the appropriate voltages to electrodes through control pins as *electrode addressing*. Early DMFB designs relied on *direct addressing*, where each electrode is *independently* addressed with a dedicated control pin [4]. This addressing maximizes the flexibility of electrode control. However, for large arrays, direct addressing leads to the problem of high pin-count demand and it is not feasible for low-cost and disposable biochips that are required for diagnostics and laboratory applications.

Designs for pin-constrained digital microfluidic biochips (PDMFBs) are receiving much attention because they simplify chip fabrication and packaging, and reduce product cost. To reduce cost and at the same time, ensure the correct sequence of correct electrode actuation, *broadcast addressing*, has been appreciated as a promising method [14]. This addressing scheme maintains high assay throughput and reduces the pin count by identifying electrodes with *compatible* control signals and merging/connecting them together. In other words, multiple electrodes are controlled by a single signal source and actuated simultaneously. Realization on a recently developed *n*-plex assay using only 64 pins to control over 1000 electrodes has been successfully commercialized [1], [11].

Although broadcast addressing serves as a promising solution to pin-count reduction, signal merging may introduce additional (and unnecessary) electrode actuations. Take Figure 2 as an example. In (a), the direct-addressing result with 3 pins makes electrodes e_1, e_2, and e_3 require 3, 2, and 3 time steps of actuations, respectively. Suppose the control signals of e_1 and e_2 are compatible. After applying the broadcast-addressing method, the pin count can be reduced to 2 pins, as shown in (b). However, this addressing result increases the number of electrode actuations of e_1 and e_2 to 5 time steps, additionally brought from sharing signals with each other. Therefore, if the broadcast-addressing solution is not carefully generated, there is the risk of excessive electrode actuations.

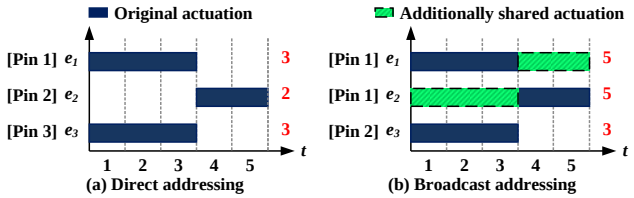

Figure 2. Broadcast addressing demands more electrode actuations than direct addressing.

Studies on PDMFBs have pointed out that excessive electrode actuations have direct and adverse effect on chip reliability. Two physical phenomena, namely *trapped charge* and *residual charge*, are of the most concern [9], [13]. Charge trapping is a phenomenon whereby charge gets trapped and concentrated in the dielectric insulator of the chip, which exerts to a reduction on electrowetting force. In the case of excessive actuations, charge trapping becomes severe, and it eventually causes permanent dielectric degradation [3]. In this scenario, droplets may be stuck and droplet movement under voltage control may no longer be possible [2]. On the other hand, overly actuating an electrode substantially increases the amount of charge that accumulates in the actuated electrode. If the next electrode is in

978-1-4577-1400-9/11/$26.00 ©2011 IEEE

turn actuated whereas the present electrode has residual charge, the droplet may not be moved toward the next direction as expected. This situation is referred to as the residual-charge problem [9]. As a result, the above two problems inevitably impede complete and correct assay execution, thereby degrading chip reliability significantly.

Reliability is a key requirement in PDMFBs, especially for medical applications such as clinical diagnostics, immunoassays, and point-of-care testing [2], [11]. These chips must guarantee reliable assay execution and outcomes as they directly influence the final medical decision making. To enhance reliability, material improvements on dielectric insulator and electrodes have been made to alleviate the impact of trapped-charge and residual-charge problems [7], [9]. Nevertheless, it has also been reported that progress in material science alone is not sufficient for many medical applications [3]. A major problem is that these applications typically include time-consuming fluidic protocols (e.g., incubation, washing, etc.), which demand a relatively high number of electrode actuations [11]. This concern becomes even more critical when pin-constrained design is involved because control-signal sharing further demands additional electrode actuations. In such cases, it is desirable to target reliability while generating a solution for electrode addressing, a design step that determines the control signals for the biochip. Despite the importance of reliability, current electrode addressing methods neglect this problem.

In this paper, we propose the first reliability-oriented broadcast-addressing algorithm for PDMFBs. We identify the causes of reliability degradation and highlight the design challenges involved. We propose general models and formulations as well as an effective and efficient algorithm to tackle the reliability-oriented broadcast-addressing problem for PDMFBs. The effectiveness of the proposed addressing algorithm is demonstrated on two commercial PDMFBs used for DNA sample preparation and *n*-plex immunoassay, respectively; these are two fundamental requirements for medical applications of point-of-care testing. Compared with a baseline method and the design fabricated for a commercial chip [1], our addressing algorithm achieves the best result in preventing PDMFBs from reliability degradation, while satisfying the pin-count specifications of these chips.

The remainder of this paper is organized as follows: Section II describes the broadcast addressing for PDMFB realization. Section III details the causes of reliability degradation and defines quantitative design models. Section IV formulates the reliability-oriented addressing problem. Section V discusses the proposed algorithm. Finally, Sections VI-VII describe our experimental results and conclusion.

II. Broadcast Addressing

Typically, droplet-control information is stored in the form of *electrode actuation sequences*. Each bit in the sequence represents an actuation status of the electrode in a specific time step, and can be represented as actuated "1", grounded "0", or don't care "X". The term "1" ("0") represents a control signal switched to actuation (grounding) status. In this paper, we quantify each "1", in a sequence as *one actuation unit*, or AU for short. The symbol "X" indicates that the input signal can be either "1" or "0", which has no impact on scheduled droplet controls [14]. To correctly drive these electrodes, control pins must be appropriately assigned to electrodes for identifying input signals. This process is also referred to as *electrode addressing*. Unlike direct addressing, which addresses each electrode with an independent pin, broadcast addressing focuses on replacing don't care terms with "1" or "0" to make multiple actuation sequences share an *identical* outcome sequence. Hence, these electrodes can share a control pin to receive the same control signal, thereby reducing the pin count.

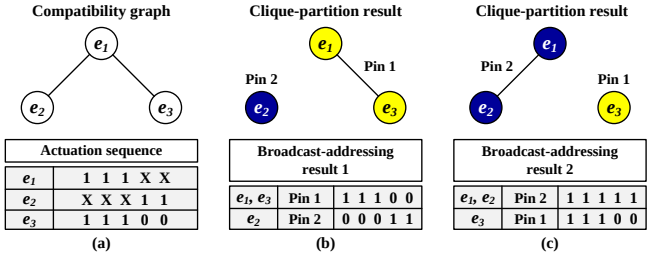

Figure 3. Illustration of broadcast addressing. (a) Three electrode actuation sequences and the derived compatibility graph. (b)-(c) Two broadcast-addressing results with both using two pins and the corresponding clique-partition graphs.

The notion of a *compatibility graph* can be used to visualize broadcast addressing. Each node in the graph represents an electrode, while an edge represents the corresponding two electrode are compatible. Based on this graph model, it has been shown that the problem of minimizing the pin count is equivalence to the classical NP-hard graph problem of minimum clique partition [14]. It is obvious that different partitions lead to different addressing results corresponding to different requirements of AUs. This feature holds true even with the same partition cardinality (i.e., the same pin count). Take Figure 3 for example. Given three electrodes e_1, e_2, and e_3 with actuation sequences "111XX", "XXX11", and "11100". These information and derived compatibility graph can be illustrated in (a). We can obtain a broadcast-addressing result with 2 pins by replacing all "X" terms in e_1 with "0" to be identical as e_3. This addressing result and the corresponding clique-partition result are illustrated in (b). Likewise, an alternative can be obtained as illustrated in (c). We observe that although both the addressing results in (b) and (c) obtain 2 pins, the total of required AUs are quite different. Compared with (c), the addressing result in (b) is more desirable as it requires a fewer number of AUs for each electrode.

III. Reliability-Oriented Design Model

Although broadcast addressing provides a good solution to pin-count reduction, inappropriate signal merging may potentially make electrodes to be excessively actuated. In this section, we highlight the influences of excessive actuations on reliability degradation, and two practical problems, namely *trapped charge* and *residual charge*, are discussed. Table I provides a summary of these problems and lists how they can be avoided.

TABLE I: CAUSES OF RELIABILITY DEGRADATION

Type/Cause	Target	Fault model	Observable error	Resolution
Trapped charge	Insulator	Electrowetting force reduction	Stuck droplet	Avoid excessive actuations
Residual charge	Electrode	Electrode remains residually actuated	Unexpected droplet operation	Insert grounding vectors

A. Trapped-Charge Problem

When we actuate the electrode to generate a potential difference between the droplet and electrode, electric forces work on the ions in the droplet and pull them toward the insulating layer. This phenomenon is the so-called electrowetting-on-dielectric (EWOD) or electrowetting force [10]. For each actuation there is a likelihood that charge becomes trapped in the dielectric insulator, as each actuation naturally induces an electric-field transition between the

metal electrode and dielectric insulator [13]. The amount of trapped charge substantially increases once the electrode is actuated for many times [3]. Trapped charge inevitably exerts an influence on electrowetting force, denoted as γ, with the following relationship (V_a and V_t respectively denote the voltage values of actuation and trapped charge):

$$\gamma \propto (V_a - V_t)^2 \tag{1}$$

As presented in (1), the electrowetting force is proportional to the square of the actuated voltage minus the trapped charge. It is clear that the trapped charge lowers the electric field generated by the electrode and thus reduces the electrowetting force. The reduction of electrowetting force makes the droplet be no longer moved under the current supply actuation voltage. Specifically, the droplet may be stuck on the electrode and thus the entire assay execution may fail, which significantly degrades the chip reliability. Although increasing the actuation voltage can alleviate this problem, this temporary solution introduces other severe problems such as trapping intensification, dielectric breakdown, and electrode burnout [3]. Therefore, an addressing solution that avoids excessive electrode actuations is more practical and effective for reducing the impact of the trapped-charge problem. Formally, it is desirable to minimize the number of required AUs of each addressed electrode.

B. Residual-Charge Problem

Excessive electrode actuations might incur prolonged actuation for some electrodes. A problem that can be encountered with prolonged electrode actuation is the residual-charge problem. For example, given two adjacent electrodes, said left and right. Suppose we have applied a long actuation duration to the left electrode until time step t. And much charge has accumulated in this electrode. If we actuated the right electrode at the next time step $t + 1$, with the present electrode *residually charged*, there may exist an ambiguous situation in moving this droplet. In other words, the droplet may be stuck on the present electrode or even be wrongly split. Considering this fault, the residual-charge problem critically prevents droplets from stable and expected movements, which potentially degrades chip reliability [9].

1) Resolution with Grounding Vectors: Unlike the trapped charge, which is basically an *irreversible* charge concentration problem, experiments have shown that residual charge can be removed by lengthening the grounding time [9]. Specifically, by switching the electrode into grounding status with enough time steps, the residual-charge problem can be avoided. To this end, in this paper we introduce the concept of the *grounding vector*, or GV for short, indicating a control signal of grounding all electrodes by additional one time step. That is, all operations are temporarily suspended by one time step for one GV insertion. Without loss of generality, we adopt a given function, denoted as $f(r)$, to represent that every r continuous AUs should be followed by at least $f(r)$ GVs. Note the fact that this continuous condition is with respect to a maximal actuation span. The use of the function is reasonable and flexible as several factors such as electrode shape, supply voltage, or switching frequency, can contribute to the degree of residual-charge problem [9]. Hence, it varies from different chips.

Take Figure 4 for example. Suppose that we are given three electrodes and their actuation sequences as shown in (a), and we are using the function $f(4)$ = 2 to avoid the residual-charge problem. Although control signals of e_1 and e_2 are compatible, their outcome (merged) sequence suffers from the residual-charge problem and thus they cannot be addressed together, as shown in (b). This is because there are only one GV and zero GV following the sixth and tenth time

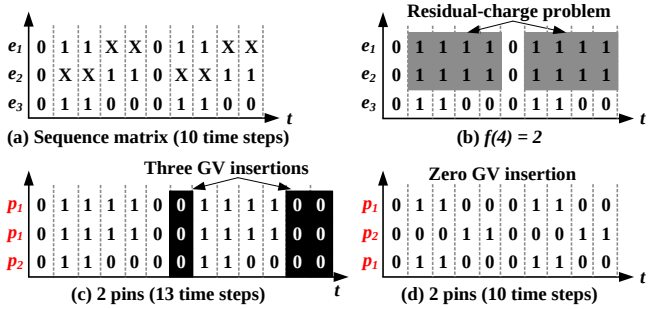

Figure 4. Residual-charge avoidance by inserting the grounding vectors (GVs) (suppose the residual-charge problem begins with four continuous actuations). (a) Three electrode actuation sequences. (b) e_1 and e_2 cannot be addressed together due to the residual-charge problem. (c)-(d) Two addressing results with both two pins and, however, different numbers of GVs.

steps, respectively, and we require two GVs for avoiding the residual-charge problem. (i.e., $f(4) = 2$). To make such an addressing feasible, we should appropriately insert 3 GVs such that e_1 and e_2 can be addressed together, as shown in (c). Apparently, different addressing solutions lead to different numbers of inserted GVs. As the same example in Figure 4, an alternative in (d) obtains the same pin count as (c). Nevertheless, (d) actually requires *zero* GV insertion and therefore, from a fluidic viewpoint, has faster assay completion time over (c). Such timing concern is of much importance for many safety- and time-critical applications requiring real-time response and rapid time-to-response [2]. Hence, it is necessary to reduce the overhead of inserted GVs.

2) Preservation of Critical Operations: Even though the insertion of GVs can avoid the residual-charge problem, the temporary suspension may adversely affect some operations that require precise timing control. For instance, on-chip droplet operations such as washing, incubation, PCR looping, DNA amplification, precise-volume dispensing, etc., have been associated with specific timing condition for reliable execution. When executing these operations, any temporary suspension caused by inserting GVs is prohibited. In this paper, we referred to these kinds of operations as *critical operations*.

An example of a critical operation is the incubation in an immunoassay protocol [11]. During the incubation, a blood droplet with antibodies and magnetic beads are shuttled or subjected to a series of splitting and merging operations around a linear electrode pathway to improve binding efficiency. Since a specific number of time steps has been experimentally associated to carry out a stable and reliable incubation (e.g., in this example, it takes 630 seconds or 630 time steps with 1 Hz switching frequency to complete the binding), any temporary suspension caused by inserting GVs is prohibited. Therefore, electrode addressing must be carefully performed to deal with this concern while avoiding the residual-charge problem.

IV. Problem Formulation

Based on previous discussions, the reliability-oriented design problem of PDMFBs can be formulated as follows:

Input: *An electrode set E_e with the corresponding actuation sequences and specifications of P_{max} and $f(r)$.*

Constraints:

1) Pin constraint: *The pin count used for electrode addressing cannot exceed the maximum allowable number, P_{max}.*
2) Broadcast-addressing (BA) constraint: *Given an electrode set, if the corresponding actuation sequences are mutually compatible, this electrode set can be addressed with the same*

control pin or not; otherwise, it cannot be addressed with the same control pin.

3) Residual-charge-avoidance (RCA) constraint: *During the signal merging, every r maximally continuous AUs should follow by $f(r)$ GVs.*
4) Critical-operation-preservation (COP) constraint: *Given a set of critical operations, the corresponding execution time steps in electrode actuation sequences should be preserved and disallow the insertion of GVs.*

Objective: *Deriving a correct and reliable electrode-addressing result while keeping the number of required AUs of each addressed electrode as minimum as possible. Under the above constraints, the number of inserted GVs should be minimized so as to reduce the impact on assay time-to-response.*

A. Formal Problem Statement

To be precise and clear, we mathematically model the objective mentioned above. We define two parameters as follows: (1) AU_k represents the required AUs in the actuation sequence of electrode e_k, and (2) AU_{max} represents the maximum value among AU_k for all e_k. An example of calculating these two parameters can be demonstrated in Figure 5.

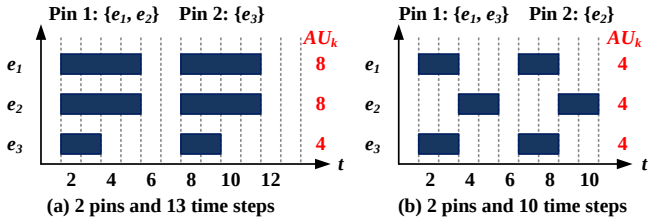

Figure 5. Time charts corresponding to Figure 4(c)-(d). (a) $AU_1 = 8$, $AU_2 = 8$, $AU_3 = 4$; $AU_{max} = 8$. (b) $AU_1 = 4$, $AU_2 = 4$, $AU_3 = 4$; $AU_{max} = 4$.

Based on the above definitions, the original objective can be mathematically restated as follows: *Derive a correct electrode-addressing result with minimized AU_{max}. With this global minimization objective, minimize each AU_k and the total number of inserted GVs.*

V. Algorithm

Before introducing our algorithm, we highlight a key yet obvious observation from the problem formulation as follows:

Lemma 1: Let L denote the length of original actuation sequences. The upper bound and lower bound of AU_{max} are given by 0 and L, respectively.

The above lemma makes it possible to leave aside the regular problem-solving perspective posed by directly optimizing the original addressing problem, which is usually intricate and complicated. We come up with an idea that transforms the original optimization problem into a *deterministic problem*, in which a deterministic constraint specifying the upper bound of AU_{max} is imposed. This transformation greatly facilitates the entire problem-solving process as now we can narrow down our effort to focus on only dealing with theses constraints. To this end, we intend to derive a general model through which all constraints can be routinely modeled with each iteration of adjusting the deterministic constraint.

A. Deterministic Addressing Problem Formulation

Instead of directly solving the original optimization problem, we target the following deterministic addressing problem.

Input: *An electrode set E_e with the corresponding actuation sequences, specifications of P_{max} and $f(r)$, and a determined value of AU_{max} (i.e., AU_{max} is now specified).*

Constraints: *In addition to pin, BA, RCA, and COP constraints, we have a new constraint, called deterministic constraint, to restrict that the resulted AU_k of each electrode e_k cannot exceed the determined value of AU_{max}.*

Objective: *Determine a binary feasibility of whether an addressing solution satisfying all constraints exists.*

For purpose of solving the deterministic addressing problem (i.e., examine the feasibility) efficiency, the entire addressing problem is divided into several small subproblems. We progressively solve each subproblem one by one and maintain a minimum pin-count growth between successive subproblems (will be detailed in sections V-A1 and V-A2). In each subproblem, we propose a matching-based algorithm that can *exactly* formulate design constraints into a weighted bipartite-matching problem (will be detailed in section V-A3). Finally after the addressing problem is solved, we examine the resulted pin count and check whether it exceeds the pin constraint. If it fails to satisfy the pin constraint, we know that the specified value of AU_{max} is infeasible to hold a correct addressing solution; otherwise it is feasible to hold a correct addressing solution.

1) Progressive Addressing Framework: As modern PDMFBs may contain thousands of electrodes, it is computationally costly to handle the addressing problem directly. Motivated from [6], we propose a progressive addressing framework based on *pin-count expansion* to reduce the design complexity. Figure 6 illustrates the essential concept of the proposed progressive addressing framework.

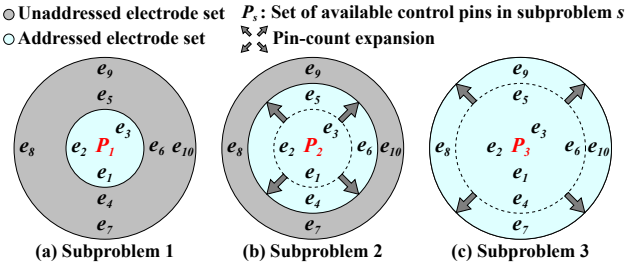

Figure 6. The concept of our progressive addressing framework.

The main idea is to divide the original problem into a set of manageable subproblems corresponding to each pin-count expansion. In each subproblem, the entire electrode set is decomposed into two subsets, a unaddressed electrode set and an addressed electrode set (see Figure 6(a)). Or, in other words, a unaddressed electrode set and an existing pin set. The objective of solving each subproblem is to derive an addressing result while making extra pin-count demand as minimum as possible. After that, the pin count is progressively expanded with the addition of extra pin-count demand and the addressing procedure seamlessly proceeds into the subsequent subproblem (see Figure 6(b)). Then, expansion ends until all electrodes are addressed (see Figure 6(c)). Finally, we examine the feasibility of the given deterministic addressing problem.

2) Modeling the Pin-Count Expansion: Essentially pin-count expansion describes the concept of *extra* pin-count demand that must be included to complete the electrode addressing for a subproblem s. To comply with the pin constraint, we should avoid pin-count overhead and minimize expansion size. Hence, the means by which the set of *existing control pins* in a subproblem s, denoted as P_s, can be *maximally* utilized for addressing is the major concern in modeling

the pin-count expansion.

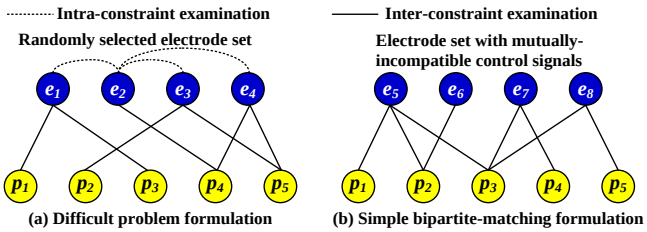

Figure 7. Motivation of electrode selection to formulate the pin-count expansion problem. (a) Randomly selecting an electrode set. (b) Selecting an electrode set E'_e with mutually-incompatible control signals.

The major difficulty in solving each subproblem s is to select a unaddressed electrode set for addressing. The selection method greatly affects the design complexity in formulating and solving the pin-count expansion. As shown in Figure 7(a), if we neglect this concern and apply a random selection, many constraints (i.e., intra and inter) need to be examined. Hence, the problem is hard to be efficiently and effectively formulated. To tackle this problem, we reverse the regular electrode selection method which is based on compatible signal identification. Specifically, we select a maximum unaddressed electrode group, denoted as E'_e, with mutually *incompatible*, rather than compatible control signals. As shown in Figure 7(b), this strategy significantly reduces the complexity and facilitates the problem formulation. This is because electrodes inside E'_e are mutually-incompatible and thus we can omit the intra-constraint examination inside E'_e. In this manner, the addressing problem can be effectively formulated to a *one-to-one* matching determination between the two sets E'_e and P_s.

After E'_e is identified and selected, the major goal is to correctly derive an addressing result, while keeping the number of control pins and inserted GVs minimized. Since all electrodes $e_k \in E'_e$ must be independently addressed, once the addressing procedure is finished, each of the rest and unaddressed electrode $e'_k \in E'_e$ necessitates an *extra/independent* pin, implying *pin-count expansion*. In order to avoid pin-count overhead, it is desirable to *maximally* utilize the existing control pins $p_i \in P_s$ for addressing, such that the pin-count expansion can be minimized. Furthermore, the number of inserted GVs needs to be minimized so as to reduce the time-to-result effect. As a consequence, for each subproblem s, the problem of pin-count expansion can be formulated as follows:

Input: *Given two sets, E'_e and P_s.*

Constraint: *All constraints listed in the deterministic addressing problem formulation, section V-A, must be satisfied.*

Objective: *Maximally utilizing P_s for addressing E'_e to minimize the pin-count expansion, while keeping each AU_k and the total number of inserted GVs minimized.*

Note that E'_e can be obtained by searching the maximum independent set of the compatibility graph, where a number of high quality heuristics can be adopted to solve it [14] .

3) Minimum-Weight Bipartite-Matching Formulation: We construct a minimum-weight bipartite-matching (MWBM) graph $G_{mwbm} = (V_{mwbm}, E_{mwbm})$ to solve the problem of pin-count expansion. The node set V_{mwbm} consists of two disjoint partite sets, V^e_{mwbm} and V^p_{mwbm}. We also propose two formulation rules. The first rule describes the formulation of V_{mwbm}, and the second rule describes the formulation of E_{mwbm}.

The key idea behind our MWBM formulation is to map the objective "*maximally utilizing P_s for addressing E'_e*" into "*maximum matching value*" in G_{mwbm}, with "*keeping each AU_k and the total number of inserted GVs minimized*" corresponding to "*minimum matching cost*". Considering the compatibility, we define the control pin set $P^k_s \in P_s$ for each electrode $e_k \in E'_e$ to identify the control pin $p_j \in P^k_s$ being compatible with e_k. P^k_s can be easily obtained by simply checking the legality of all constraints for any pair (e_k, p_j). In another aspect, all constraints can be easily formulated in a fashion of graph connection, which is attributed to the proposed MWBM formulation. Take Figure 8 for instance. Given a subproblem s with $AU_{max} = 5$, $f(3) = 2$, and a critical operation occurring from the third to fifth time step. Take e_1 for example, we can address e_1 with p_2 by inserting one GV (i.e., following the sixth time step to be "10111001"). However, we cannot address e_1 with p_1 as such addressing requires one GV insertion following the fourth time step, which violates the COP constraint. Hence, we have $P^1_s = \{p_2\}$. Another notable example is the illegality of addressing e_2 with p_3, whose outcome sequence, "0111111", has 6 AUs and violates the deterministic constraint ($AU_{max} = 5$). Accordingly, we have $P^2_s = \{p_1, p_2, p_4\}$. By repeating the examination procedure, we could identify the compatibility between E'_e and P_s as the matrix shown in Figure 8. Each entry (k, j) in the matrix headed by T/F represents that e_k can/cannot be addressed with p_j.

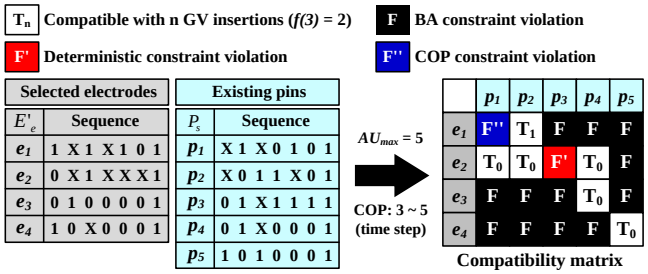

Figure 8. An example of identifying the compatibility in a subproblem s.

Based on these definitions, the two MWBM formulation rules can be presented as follows:

MWBM-Rule #1 - Formulation of V_{mwbm}:

- V^e_{mwbm}: For each electrode $e_k \in E'_e$, create a node v_{e_k}.
- V^p_{mwbm}: For each control pin $p_i \in P_s$, create a node v_{p_i}.

MWBM-Rule #2 - Formulation of E_{mwbm}: The edge formulation consists of two steps. In the first step, we establish an edge connection for each node pair (V_{e_k}, V_{p_j}), $e_k \in E'_e$ and $p_j \in P^k_s$. In the second step, each established edge is associated with an addressing cost, denoted as $cost(e_k, p_j)$, which is defined as follows:

$$cost(e_k, p_j) = \alpha \cdot AU_{e_k \to p_j} + \beta \cdot GV_{e_k \to p_j} \quad (2)$$

Where $AU_{e_k \to p_j}$ and $GV_{e_k \to p_j}$ respectively denote the numbers of required AUs and inserted GVs in addressing e_k with p_j. And α and β are user-specified parameters. In this paper we set $\alpha = 10$ and $\beta = 1$. Note that the calculation of $AU_{e_k \to p_j}$ should include those electrodes which are pre-addressed with p_j. For example, in Figure 8, the outcome sequence of addressing e_1 with p_2 is "10111001" (including one GV). Suppose there is one electrode pre-addressed with p_2. Then we have $AU_{e_1 \to p_2} = 5 \times 2 = 10$ and $GV_{e_1 \to p_2} = 1$. Based on the proposed MWBM formulation rules, we have the following two theorems and one lemma.

Theorem 1: Each matched edge in the MWBM graph represents a correct electrode addressing.

Theorem 2: Based on the proposed MWBM formulation, we can adopt the MWBM algorithm to optimally maximize the number of addressed electrodes with minimum total addressing costs.

Lemma 2: The extra pin-count demand for electrode addressing is equal to $|E'_e| - N_{mwbm}$, where N_{mwbm} denotes the maximum matching value in G_{mwbm}.

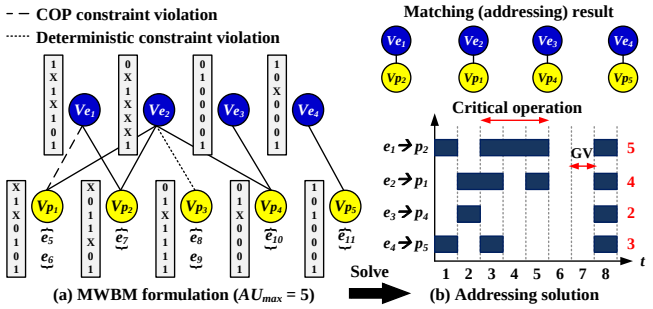

Figure 9. MWBM formulation derived from Figure 8.

Figure 9 depicts the MWBM formulation derived from Figure 8. After solving the MWBM, we could obtain 4 matched pairs, (e_1, p_2), (e_2, p_1), (e_3, p_4), and (e_4, p_5), which actually map to 4 electrode-addressing results. Note that addressing e_1 with p_2 introduces one GV insertion. In this case since all selected electrodes are successfully addressed (i.e., by maximally utilizing existing control pins), the expansion size of pin count is minimized to zero. In other words, no extra control pins are demanded to solve this addressing subproblem. In addition, minimum matching cost can also keep the numbers of required AUs and inserted GVs among these addressed electrodes minimized.

B. Iterative-Incrementing Search Technique

Based on the proposed algorithm to solve the deterministic problem, we observe a property that the edge density is highly-concerned with the matching outcome. A dominating factor on edge density comes from the specified value of AU_{max}, as a lower AU_{max} has more tight restriction on establishing edge connection than a higher one. Accordingly, increasing AU_{max} can increase the edge density thereby generating more matched pairs. This feature implies that an MWBM solution with higher AU_{max} may have more electrodes addressed with existing pins, and thus a smaller pin-count expansion to minimize the total pin count than that with lower AU_{max}. As in our progressive addressing algorithm the total pin count is a decisive factor on examining the feasibility of a deterministic problem. With the above discovery that incrementing AU_{max} may facilitate pin-count reduction, if the present deterministic problem returns an infeasible situation, we intend to increment AU_{max} and re-examine it again. Regarding the lemma 1 and the fact that we want to minimize AU_{max} for better reliability, an iterative-incrementing search strategy can be conducted to realize this objective. In our iterative-incrementing search technique, we first initialize AU_{max} to be the maximum value among all AU_k before addressing. Then the proposed search technique runs repeatedly, incrementally lengthens AU_{max} by one with each iteration, examining the feasibility by our progressive addressing algorithm and finally ends until it meets a feasible condition. Note that in case of a failure addressing, it should be resorted to the early design stage for resolution such as operation re-synthesis [8], [12], whereas this issue is beyond the scope of this paper.

VI. Experimental Results

We implement the proposed addressing algorithm in C++ language on a 2-GHz 64-bit Linux machine with 16GB memory. Two commercial PDMFBs for DNA sample preparation and *n*-plex immunoassay are used for experimental evaluation [1]. The two chips are considered for point-of-care testing and involve typical fluidic protocols that are used for many healthcare-related assays. Reliability here is a fundamental requirement as any fluidic error or physical defect directly affects medical diagnosis. The function $f(r)$ is set as $r/11+1$ for avoiding residual-charge problem [9]. To demonstrate the effectiveness of our addressing algorithm for reliability enhancement, addressing results are considered for a baseline method and two fabricated commercial biochips described in [1]. Note that we have access only to the electrode-addressing result data for the commercial *n*-plex biochip; other details about the chip are not available for public disclosure due to intellectual property reasons. We implement the baseline method as follows: Procedure consists of $|E_e|$ iterations, where $|E_e|$ denotes the total number of input electrodes. In each iteration, we randomly select a unaddressed electrode and identify an existing pin (i.e., with respect to addressed electrodes) that can be correctly assigned to this electrode. If no such a pin exists, we additionally assign an independent control pin to this selected electrode.

A. Commercial PDMFB for DNA Sample Preparation

The extraction of DNA from raw physiological sample of human whole blood is a critical step for any point-of-care DNA analysis. Whole blood has a very high load of cells and therefore a large amount of sample is generally not required for human genomic DNA-based testing. In order to extract high-quality and purified human genomic DNA from whole blood, a simple yet effective PDMFB for DNA sample preparation has recently been developed [1].

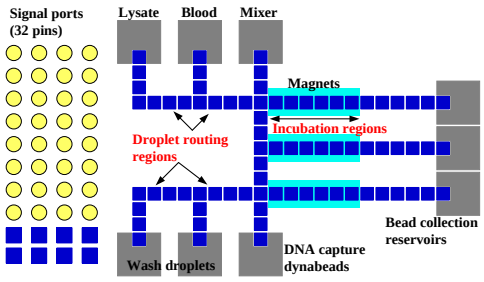

Figure 10. Layout of a PDMFB used for DNA sample preparation with extraction of human genomic DNA from whole blood.

The schematic layout of the chip is presented in Figure 10. The chip is based on a pin-constrained design that comprises 86 electrodes with a limited number of 32 signal ports. We consider DNA extraction, where control signals are given to perform the following operations sequentially: (1) droplets with whole blood and lysate are dispensed from reservoirs and transported to the mixer for cell lysis; (2) droplets with lysated cells and DNA capture dynabeads are dispensed from reservoirs and transported to incubation regions for bead binding; (3) wash droplets are then used to elute the beads to remove cell debris; (4) purified genomic DNA captured on the beads is then collected at bead collection reservoirs. The entire execution consumes 746 time steps and there are two types of on-chip critical operations (totally six critical operations) of incubation and washing, which take 450 and 120 time steps, respectively.

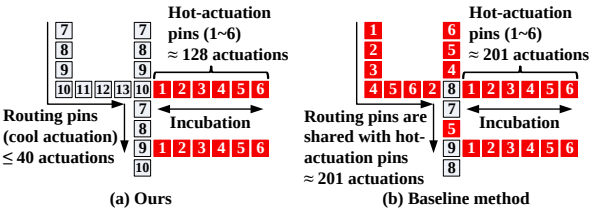

Figure 11. Addressing-solution fragments of ours and baseline method. Hot-actuation pins are: (1) localized; (2) spread out.

Next we use the proposed algorithm and baseline method to obtain the electrode addressing results. Figure 11 shows the fragments of addressing solutions obtained by our approach and the baseline method. We observe that on-chip protocols for incubation and washing demand a relatively high number of electrode actuations compared to other other operations such as routing and merging. We refer to those control pins (i.e., pins $1 \sim 6$), which are assigned to execute these protocols, as *hot-actuation pins*. In (a), our addressing algorithm lets electrodes addressed with hot-actuation pins be localized in incubation regions. However, the baseline method in (b), based on unrestricted sharing of control pins/signals, spreads out the hot-actuation pins to other electrodes; for example, electrode pathways used for droplet routing. In such a way, when the incubation or washing is being executed, many electrodes that are not relevant will be unnecessarily and excessively actuated.

TABLE II: COMPARISON BETWEEN BASELINE AND PROPOSED METHOD

Chip	Baseline					Proposed method				
DNA sample preparation	AU_{max}	AU_{avg}	#GV	#Pin	CPU(s)	AU_{max}	AU_{avg}	#GV	#Pin	CPU(s)
	201	130	24	16	0.24	128	40	0	22	0.44

AU_{max}: the maximum resulted number of electrode actuations #Pin: the number of control pins
AU_{avg}: the average number of electrode actuations #GV: the number of inserted grounding vectors

Table II reports the comparison result between the baseline method and our addressing algorithm. First, the quantitative values of AU_{max} and AU_{avg} show that we achieve 36.3% and 69.2% reductions in comparison to the baseline method, respectively. This result shows that our addressing algorithm minimizes the peak number of required actuations as well as maintaining a relatively low number of actuations for all electrodes, thereby reducing the trapped-charge effect significantly. Second, we can see that our addressing algorithm avoids residual-charge error without any GV insertion, whereas the baseline method results in 24 GVs. Thereby, we can avoid timing overhead for assay execution. Third, an increase in pin count is expected as we incorporate several reliability-improvement constraints in the electrode addressing. However, our addressing result, using fewer than 32 pins, still satisfies the pin constraint. Overall, these results demonstrate the effectiveness of our addressing algorithm on improving reliability in the design of PDMFBs.

B. Commercial PDMFB for n-plex Immunoassay

The *n*-plex immunoassay is a typical example of a multiplexed and high-throughput bioassay. In this assay, sample droplets are mixed with *n* different reagents, the mixed product droplets undergo incubation, then are transported to a detection site. The layout of the commercial PDMFB for *n*-plex immunoassay is presented in Figure 12 [1]. The chip consists of 1140 electrodes and 64 control pins; hence it is large enough to demonstrate the scalability of our addressing algorithm.

We demonstrate a 4-plex heterogeneous sandwich immunoassay based on handling of magnetic beads [11]. Control signals are given to perform the following operations: (1) a total of 12 sample

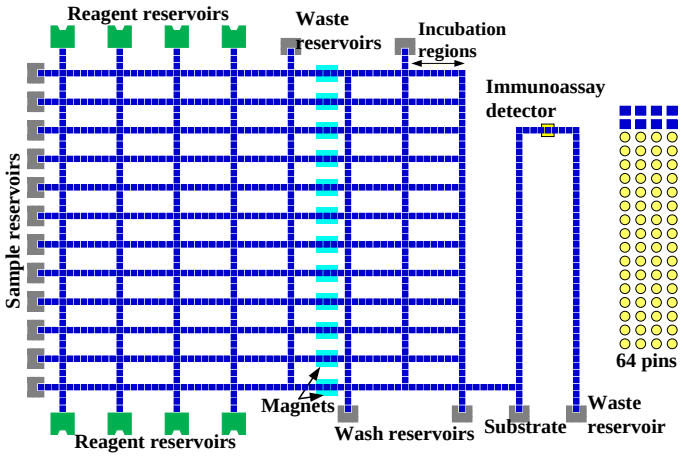

Figure 12. Layout of a PDMFB used for *n*-plex immunoassay.

blood droplets are dispensed and merged with three types of reagent droplets: reagent droplets containing magnetic beads with primarily captured antibodies; reagent droplets containing reporter antibodies labelled with alkaline phosphatase (ALP); reagent droplets containing analyte for antibody-antigen-reporter binding; (2) merged droplets undergo incubations; (3) then, incubated droplets are transported to magnet sites for washing and purification; (4) purified droplets are then mixed with chemiluminescent reagents through incubations; (5) product droplets are transported to the detection site for detection and collected in the waste reservoir eventually. The entire execution consumes 1586 time steps with two types of critical operations (totally 36 critical operations), incubation and washing protocol. The incubation of antibody-antigen-reporter binding takes 630 time steps, the washing protocol takes 120 time steps, and the incubation of chemiluminescent mixing takes 240 time steps.

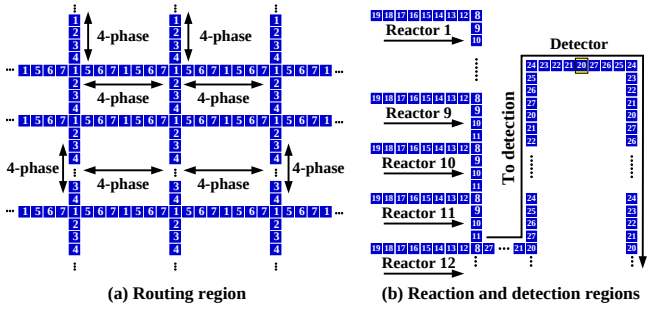

Figure 13. Manual electrode-addressing result in [1].

The electrode addressing of the fabricated *n*-plex chip is done manually by manufacturers, who empirically use a k-phase connection for the droplet pathways. Every k^{th} electrode in a k-phase bus is addressed with the same pin, where k is an empirical number varying from different chips. To avoid excessive signal sharing, manufacturers categorize the entire electrode set into three types of regions: routing region, reaction region, and detection region. Electrodes in different regions are addressed with separate sets of control pins. Figure 13 demonstrates the manual electrode-addressing result (i.e., fabricated commercial design) from [1].

For fair comparison, we conduct our addressing algorithm separately for the three regions. The overall comparison results are listed in Table III. Note that our addressing result is the same as that of fabricated commercial design in detection region and both the

TABLE III: COMPARISON BETWEEN FABRICATED COMMERCIAL DESIGN AND PROPOSED METHOD

n-plex chip	Fabricated commercial design				Proposed method				
	AU_{max}	AU_{avg}	#GV	#Pin	AU_{max}	AU_{avg}	#GV	#Pin	CPU(s)
Routing region	238	221	0	7	192	178	0	8	6.54
Reaction region	548	447	0	19	312	246	0	30	8.13
Detection region	72	31	0	8	72	31	0	8	0.47

AU_{max}: the maximum resulted number of electrode actuations
AU_{avg}: the average number of electrode actuations
#Pin: the number of control pins #GV: the number of inserted grounding vectors

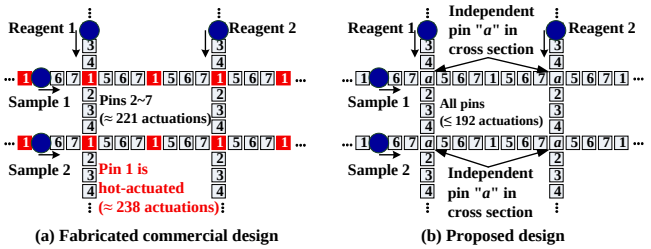

Figure 14. Comparison in routing region.

fabricated commercial design and our addressing algorithm achieve zero GV insertion. Figure 14 shows the addressing result obtained by fabricated commercial design and ours in the routing region. From our addressing result, we observe that crossing electrodes by horizontal and vertical pathways demand a relatively higher number of actuations than others. This is because crossing electrodes provide controls for both horizontally moved sample droplets and vertically moved reagent droplets. However, this subtle yet significant concern is hard to be recognized manually and therefore in the fabricated commercial design crossing electrodes are addressed together with other non-crossing electrodes by pin 1, as shown in (a). In this way, the mutually superimposed actuations make pin 1 be hot-actuated. On the contrary in (b), our addressing algorithm automatically discovers this problem and assigns an independent pin for crossing electrodes, therefore reducing AU_{max} and AU_{avg} by 19.3% and 19.5%, respectively.

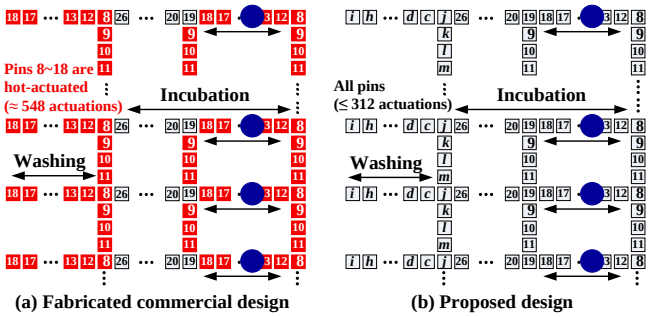

Figure 15. Comparison in reaction region.

Likewise in the reaction region, as shown in Figure 15(a), the fabricated commercial design connects the electrodes on washing region and incubation region together (i.e., including the corresponding vertical pathways) with pins 8 $\sim$ 18. When washing operations are performed, electrodes on incubation region are inevitably and additionally actuated, and vice versa. Therefore, these pins suffer from hot-actuation problems. In (b), our algorithm avoids this problem by breaking such an excessive pin sharing through addressing electrodes on washing region with independent pins, therefore reducing AU_{max} and AU_{avg} by 43.1% and 45.0%, respectively.

In summary, our algorithm satisfies all required constraints, while achieving a relatively low number of required electrode actuations in comparison to the fabricated commercial design. Besides, we observe that our addressing algorithm automatically and acutely resolves not only apparent but also subtle yet significant addressing problems, which have the potential to cause excessive electrode actuations as well as reliability degradation. Overall, all the above discussion and experimental results highlight the effectiveness of the proposed reliability-oriented electrode-addressing algorithm.

VII. Conclusion

In this paper, we have presented a novel matching-based broadcast electrode-addressing algorithm for PDMFBs to deal with the involved reliability problem in pin-constrained design. We have identified the causes of reliability degradation and introduced a new and practical formulation of reliability-oriented electrode-addressing. By incorporating the properties that are favorable for reliability enhancement into our addressing algorithm, the reliability-oriented pin-constrained electrode-addressing problem can be effectively solved. Two commercial PDMFBs of point-of-care testing, namely DNA sample preparation and *n*-plex immunoassay, have been used to evaluate the effectiveness of our addressing algorithm on preventing pin-constrained design from reliability degradation.

Acknowledgment

This work was partially supported by the National Science Council of Taiwan ROC under Grant No. NSC 100-2220-E-006-016 and in part by the US National Science Foundation under grant No. CCF-0914895. The authors would like to thank Yang Zhao and Advanced Liquid Logic, Inc., for providing details about fabricated biochips for experimental evaluation.

References

[1] Advanced Liquid Logic, Inc., http://www.liquid-logic.com.
[2] K. Chakrabarty, "Towards fault-tolerant digital microfluidic lab-on-chip: defects, fault modeling, testing, and reconfiguration," *Proc. IEEE ICBCS*, pp. 329–332, 2008.
[3] A. I. Drygiannakis, A. G. Papathanasiou, and A. G. Boudouvis, "On the connection between dielectric breakdown strength, trapping of charge, and contact angle saturation in electrowetting," *ACS J. Langmuir*, no. 25, pp. 147–152, 2009.
[4] J. Gong and C. J. Kim, "Direct-referencing two-dimensional-array digital microfluidics using multilayer printed circuit board," *IEEE J. MEMS*, no. 2, pp. 257–264, 2008.
[5] T.-Y. Ho, J. Zeng, and K. Chakrabarty, "Digital microfluidic biochips: A vision for functional diversity and more than Moore," *IEEE/ACM ICCAD*, pp. 578–585, 2010.
[6] T.-W. Huang, S.-Y. Yeh, and T.-Y. Ho, "A network-flow based pin-count aware routing algorithm for broadcast electrode-addressing EWOD chips," *IEEE/ACM ICCAD*, pp. 425–431, 2010
[7] A. Kerber, F. Cartier, R. Degraeve, P. J. Roussel, L. Pantisano, T. Kauerauf, G. Groeseneken, H. E. Maes, and U. Schwalke, "Charge trapping and dielectric reliability of SiO2-Al2O3 gate stacks with TiN electrodes," *IEEE Trans. on Electron Devices*, no. 50, pp. 1261–1269, 2003.
[8] C. C.-Y. Lin and Y.-W. Chang, "ILP-based pin-count aware design methodology for microfluidic biochips," *Proc. IEEE/ACM DAC*, pp. 258–263, 2009.
[9] J. K. Park, S. J. Lee, and K. H. Kang, "Fast and reliable droplet transport on single-plate electrowetting on dielectrics using nonfloating switching method," *J. Biomicrofluidics*, no. 4, 2010
[10] M. G. Pollack, A. D. Shenderov, and R. B. Fair, "Electrowetting-based actuation of droplets for integrated microfluidics," *Lab on chip*, pp. 96–101, 2002.
[11] R. Sista, Z. Hua, P. Thwar, A. Sudarsan, V. Srinivasan, A. E. Eckhardt, M. Pollack, and V. Pamula, "Development of a digital microfluidic platform for point of care testing," *Lab on chip*, no. 8, pp. 2091–2104, 2008.
[12] F. Su, K. Chakrabarty, and R. B. Fair, "Microfluidics based biochips: Technology issues, implementation platforms, and design-automation challenges," *IEEE TCAD*, pp. 211–223, 2006.
[13] H. J. J. Verheijen and M. W. J. Prins, "Reversible electrowetting and trapping of charge: model and experiments," *ACS J. Langmuir*, no. 15, pp. 6616–6620, 1999.
[14] T. Xu and K. Chakrabarty, "Broadcast electrode-addressing for pin-constrained multi-functional digital microfluidic biochips," *Proc. IEEE/ACM DAC*, pp. 173–178, 2008.